AUT Journal of Electrical Engineering

AUT J. Elec. Eng., 55(3) (Special Issue) (2023) 365-376
DOI: 10.22060/eej.2023.22102.5512

Three-Dimensional RF Source Localization Using Reflection and an Improved Particle Filter

S. Haidari*, A. Hosseinpour

Department of Electrical Engineering, Faculty of Engineering, University of Zabol, Zabol, Iran

ABSTRACT: This study uses an obstacle map for three-dimensional radio frequency (RF) source localization with reflection. The received signal strength indicator (RSSI) and the angle of arrival (AOA) are the observation requirements for the three-dimensional localization. In the first step of the localization, an unmanned aerial vehicle (UAV) is used to obtain AOA and locate the three-dimensional reflection using a two-dimensional map. Then, the path loss function is used and the reflection angle alongside the distance between the receiver and RF source is estimated based on RSSI. This information is integrated with the information from the two-dimensional map to estimate the RF source location in the three-dimensional space. The possible RF source locations in three-dimensional space are obtained, and it is shown that the possible locations of the RF source for one reflection in the three-dimensional make a circle, so three reflections are required for three-dimensional RF source localization. An improved particle filter is used to estimate RF source location while using the Kullback-Leibler distance (KLD) criteria and local search to improve the method performance with proper estimation speed and accuracy. The simulation results show that the improved particle filter has an adequate estimation with optimal particle number and higher execution speed than the initial particle filter.

Review History:

Received: Jan. 17, 2023
Revised: Jul. 07, 2023
Accepted: Jul. 29, 2023
Available Online: Dec. 01, 2023

Keywords:

Three-dimensional localization
RF Source
Kullback-Leibler distance
Particle Filter
Reflection
UAV

1- Introduction

The ever-increasing usage of radio signal-based devices, such as mobile phones and Wi-Fi, creates many applications based on the localization of these technologies as RF sources such as search and rescue, creating location-based intelligent advertisement systems, health field applications, and others [1,2].

Outdoor search and rescue have received much attention considering that people use smartphones that can act as RF sources for localization [3]. Also, localization systems, such as ARVA [4] which has been developed for the search and rescue of injured people, transmit electromagnetic signals, and the location of injured people can be obtained using unmanned aerial vehicles (UAVs) [5]. Wireless Infrastructure over Satellite for Emergency Communication (WISCOM) aims to use and restore the Global System for Mobile Communication (GSM) for tracking rescuer teams and victims [6]. These works are generally designed for emergencies, such as avalanches and earthquakes, where phone networks are not valid, and localization using BTS towers is impossible. These methods can help the injured much faster. Such people who carry their phones outdoors and do not have access to phone networks can be localized in emergencies like deserts using their mobile phones. In these situations, UAVs are helpful for their maneuverability, so they have been widely used in localization to automate the search and rescue process. Some methods of RF source localization using UAVs are localization based on received signal strength indicator (RSSI) [7], time of arrival (TOA) [8], combinations of different variables such as TOA and angle of arrival (AOA) [9], RSSI, AOA [10], and so on.

In general, RF signals can be received by line-of-sight (LOS) or non-line-of-sight (NLOS) for localization in outdoor search and rescue operations because of the presence of obstacles. Obstacles have a minor effect on direct LOS signals, and most signals are directly received. Localization based on LOS signals is possible using standard signal propagation equations, which are used for different problems and applications [11]. The signal is not received directly in the NLOS situation because of obstacles. Using standard signal propagation and LOS equations in this situation leads to high error rates in the localization. Localization in this situation is generally performed using two methods. The first method tries to determine NLOS signals to avoid using them for localization, and the second method reduces the effect of NLOS signals by using them alongside LOS signals [12,13].

Finding LOS signals in large spaces with obstacles may take more time and search. Also, LOS signals cannot be found when there are too many obstacles, which necessitates localization with NLOS signals using specific localization and signal propagation equations. In Figure 1, the received signal is NLOS and the LOS signals are not valid.

*Corresponding author's email: s.heidari@uoz.ac.ir

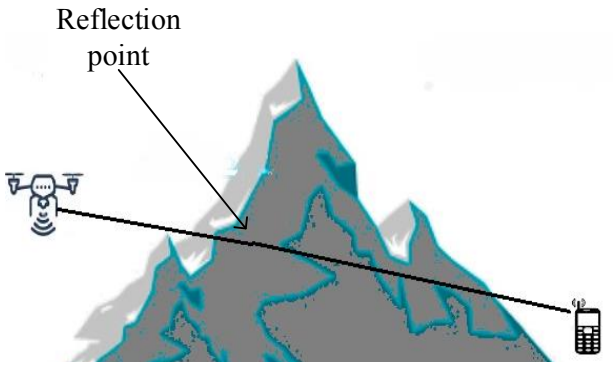

Fig. 1. An illustration of the localization using NLOS

Some previous studies conducted outdoor localization using NLOS signals. Reflection from the obstacle is one of the significant phenomena of NLOS situations that propagate these signals. Therefore, research on RF source localization has focused on reflection. These studies have considered the reflection space as an unknown location determined by observing the time difference of arrival (TDOA) and AOA [14] or RSSI and AOA [15,16]. Although the use of TOA and TDOA to estimate the distance allows for higher localization accuracy, the benefits of localization using RSSI compared to their TOA or TDOA are its simplicity of usage and lack of need for extra equipment. On the other hand, using signal times for measuring distance requires synchronicity between the radio source and receivers down to nano-seconds, which is much harder and more expensive to implement [17-18].

An important approach in NLOS localization is to use or obtain the location of the obstacle (reflection point) or a map. In [19], assuming the presence of a reflective obstacle in the environment, a moving target was localized by a reflected signal. The measured observations were TOA and AOA. This article is about obtaining the reflector location and the location of the moving target. Localization is based on the assumption of LOS between the virtual RF source and the moving target instead of the existence of NLOS between the target and the real RF source, and this method is used for moving targets. Also, the effect of other obstacles in the environment is not taken into account. In another article, localization was done by using phase fluctuations and TOA using the reflected signal. Using the geometric shape of the reflection and the characteristics obtained from the observations of the NLOS, it became a direct route and a virtual RF source, and finally, localization was done indoors [20].

In another paper, three-dimensional localization was performed indoors using reflection. The measurement was TDOA and AOA. It was assumed that a base station with a known location was available. The 3D location was estimated using this information, the reflected signal, and the LOS signal [21].

Localization using the map and reflection was conducted in [22] by a basic and advanced method and RSSI observations. The basic method had lower accuracy with a higher dependency on the geometric condition of reflectors compared to each other. At the same time, the advanced method used reflected signal propagation equations and performed its estimations using particle filters. These two methods were analytically compared using simulations, and the results showed higher localization accuracy of the advanced method.

These studies have considered an available 2D localization based on the reflected signal and map and most observations have been of TOA or TDOA type. This study localizes RF sources using a map in three-dimensional space because in the real scenario, the location of an RF source has three dimensions, so the use of 2D equations for localization in the 3D search space will be inaccurate and erroneous. So far, no research has used RSSI observations based on the reflected signal in 3D for localization using the map. We consider a simple two-dimensional map that uses AOA to determine the three-dimensional reflection location, and this information is used to estimate the three-dimensional RF source location using particle filters with local search to improve the particle weight. Also, the Kullback-Leibler distance (KLD) criterion, which helps localize robots [23], is used in the particle filter considering more complex localization estimations and equations than the two-dimensional situation and a generally wider search space. This criterion reduces the search space criteria until the estimation accuracy reaches a specific limit, the particle numbers are determined adaptively, and the particle numbers are selected comparatively with the help of this criterion over the estimation to determine the number of particles within a suitable range of accuracy and proper estimation speed.

The main contributions of this article are (1) to obtain 3D equations of the possible locations of an RF source considering the effective parameters of RSSI such as reflection angle and distance, (2) to propose a particle filtering approach for the 3D localization problem based on RSSI measurements from three reflected signals, and (3) to improve the particle filter

for 3D localization in wide search space using local search method and KLD criteria which can improve the localization accuracy with an optimum number of particles.

The rest of the article is organized as follows. Section 2 reviews the reflection signal propagation. Section 3 describes the equations of the possible locations of the RF source in the 3D and improved particle filtering approach for estimation of the location of the RF source. The simulation results are presented in Section 4, and conclusions are given in Section 5.

2- Reflection Signal Propagation

In general, signals are received directly or indirectly. The indirect signal goes through obstacles while being propagated with reflection or diffraction [18]. The signal strength of such obstacle reflection in the receiver is a function of the distance between the receiver and the RF source through the reflection path. Also, the reflector partly weakens the signal strength based on its reflection coefficient (a value between zero and one) in which one means that the obstacle fully reflects the signal without reducing its strength while zero means that it fully weakens the signal. The signal strength reduction because of its reflection path is formulated as follows [24]:

$$Path\ \ Loss = 91 + 20\log(d(KM)) - 20\log(|\Gamma(\theta)|) \qquad (1)$$

This equation is generally valid. Here, d is the reflection path length between the receiver and the RF source and θ is the reflection angle. The reflection angle is measured in three-dimensional space including the reflector, receiver, and RF source. This function shows that the changes in the signal strength reduction are caused by distance changes with a known rate. These changes can be used to calculate the distance d. On the other hand, the reflection coefficient (Γ) depends on the reflection angle. This coefficient is also dependent on the reflector surface material and ruggedness. In case there are reflective signals, we have considered the reflector as dry soil with some unevenness. Figure 2 shows the reflection coefficient changes based on different angles for the working signal of mobile phones.

3- The proposed method

We have used a GPS-equipped UAV to solve this three-dimensional localization problem to have a reading on the exact location of the UAV and direct it on any path. This UAV is also equipped with a special antenna to determine the signal AOA and RSSI. On the other hand, we assume the received signal is a reflection with proper strength. This assumption requires signals that have been reflected only once because signals with more reflections are much weaker. Also, signals with near right angles will fully disperse because of the rugged surface, so we can ignore such angles and consider a small reflection angle. Figure 3 shows a reflected signal in three dimensions.

In Figure 3, there are two angles for AOA – one is α in the (x,y) plan concerning the x-axis and the other is ϕ concerning the z-axis. This figure shows the receiving signals at the origin of coordinates for ease of use, but they could be in any location. The reflection angle θ is on a plane that passes through the receiver, RF source, and reflector. Also, is the distance between the reflector and the origin of the coordinate, and is the distance between the reflector and the RF source.

As was previously mentioned, localization is done

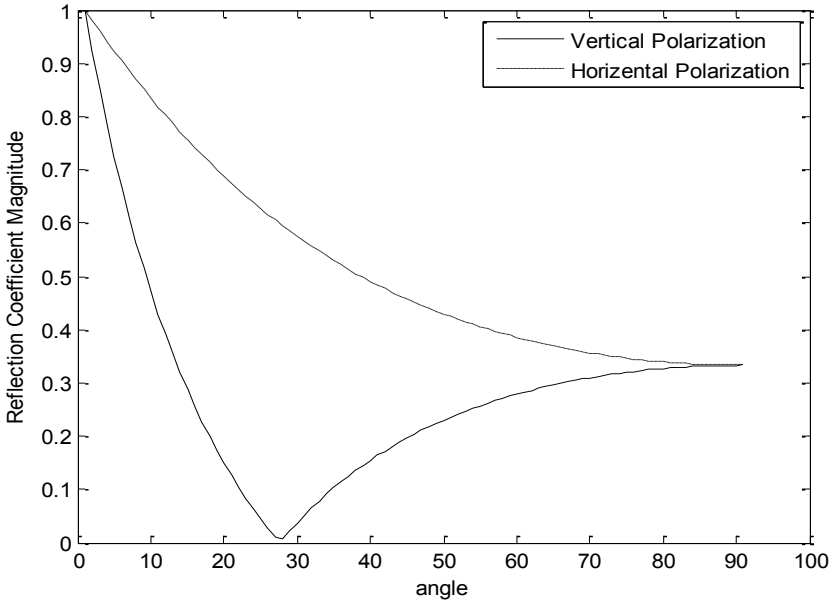

Fig. 2. Reflection coefficient magnitude for dry soil

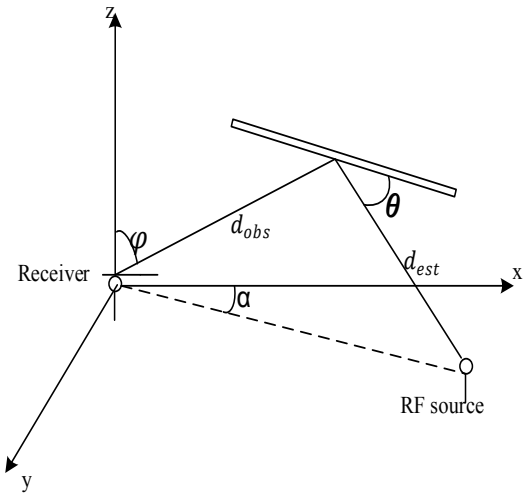

Fig. 3. The localization of the RF source is possible using reflection angle and reflection point location

according to Figure 3 with a known UAV/receiver location alongside unknown RF source and reflector locations. If we have a two-dimensional map, we can easily determine the reflector location by AOA which is shown as (x_{obs}, y_{obs}). When it comes to determining a three-dimensional location, the reflector height is calculated using the known UAV height:

$$z_{obs} = z_r - d_{pr} \tan(\varphi) \tag{2}$$

in which $d_{pr} = \sqrt{(x_{obs} - x_r)^2 + (y_{obs} - y_r)^2}$ and d_{pr} are the distance between the UAV/receiver and the reflector location in two dimensions while (x_r, y_r, z_r) is the UAV/receiver location. This equation is used to determine the reflector location in three dimensions but still, there are three unknowns (x,y,z) remaining that are related to the location of the RF source. If the UAV moves towards the signal line of the bearing, RSSI will change while the signal angle will still be the same.

Based on Equation 1, these RSSI variations are caused by the distance variation between the receiver and RF source. Therefore, we could estimate the distance between the UAV and RF source by measuring these RSSI variations caused by the known UAV movements. The distance between the RF source and the reflector is estimated using the known distance between the receiver and the reflector obstacle. This parameter alongside the reflector location shows that the RF source is on a sphere with the reflector as its center. This method could be used in situations with four reflections because the intersection of every two spheres creates a circle and these four spheres can create three circles that pinpoint the RF source location with their intersection.

Equation 1 can be used to create a better method that properly uses the current RF signal information with fewer reflections in three-dimensional localization when the reflection angle and the distance between the receiver and the RF source are known. This will create a cone-like shape for possible RF source location with the reflector in its tip just like Figure 4. This type of localization requires at least three reflections because their three-dimensional intersection determines the RF source location.

To obtain the possible RF source location equations which are mentioned above, Equation 3 can be used to determine the RF source location:

$$(x - x_{obs})^2 + (y - y_{obs})^2 + (z - z_{obs})^2 = {d_{est}}^2 \tag{3}$$

which is the sphere surface. The RF source location in the intersection equation must match the general plane equation like Equation 4:

$$ax + by + cz = p \tag{4}$$

This plane has the following normal vector:

$$\mathbf{n} = \begin{pmatrix} \cos\alpha\cos\varphi(\cos\alpha - \cos(\varphi - 2\theta)) \\ \sin\alpha\cos\varphi(\cos\varphi - \cos(\varphi - 2\theta)) \\ \cos\varphi(\sin\varphi - \sin(\varphi - 2\theta)) \end{pmatrix}$$

in which *a*, *b*, and *c* are the first to third entries of the vector. Also, a point on this plane is equal to

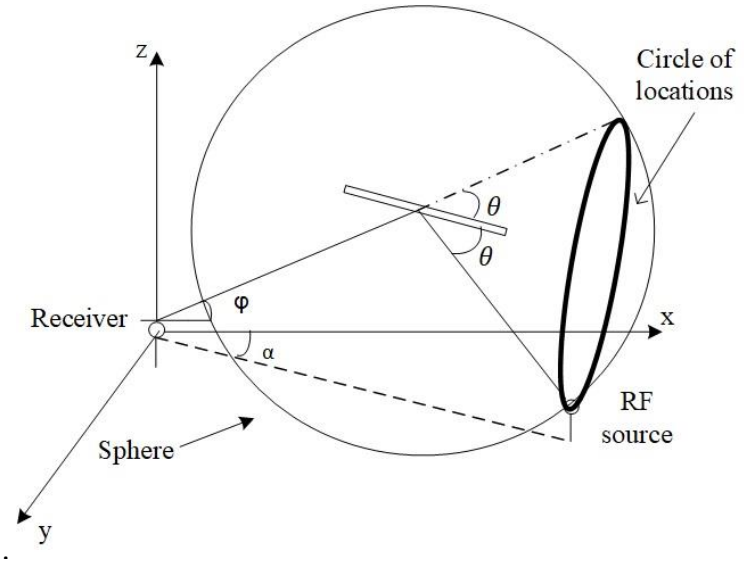

Fig. 4. The RF source locus in 3D is a circle

$$\mathbf{v}=\begin{pmatrix} x_{obs}+d_{est}\cos\alpha\sin\varphi \\ y_{obs}+d_{est}\sin\alpha\sin\varphi \\ z_{obs}+d_{est}\cos\varphi \end{pmatrix}$$

finally, p in Equation 4 can be calculated by Equation 5:

$$p=\mathbf{n}.\mathbf{v} \tag{5}$$

These equations are written with a known reflector location and AOA (the α and ϕ). Also, d_{est} and θ are estimated by Equation 1 and RSSI observations. As is evident, the possible three-dimensional RF source location points require solving some non-linear equations. This localization problem can be solved using the non-linear least-squares method. These signal propagation and localization equations are rather complex, and using non-linear optimization methods such as the non-linear least-squares method will create great dependence on the initial conditions. This article uses the adaptive improved particle filter method for estimation because it does not have the above estimation problems alongside the use of UAV for collecting RSSI and AOA samples online.

3- 1- Improved Particle Filter for Outdoor Three-Dimensional Estimation

The particle filter is used to estimate the RF source location. The state or particle variable is the RF source location and the i-th particle is $X^i=(x^i,y^i,z^i)$. The particle filter has the following steps:

• Particle initialization:

The initial particle value is determined by the highest and lowest search location dimensions in uniform distribution.

• Predicting the next phase and creating multiple particles for each particle:

We assume that the UAV flies on a specific path in a known direction and manner. A small random value is added to the particle because the RF source location is estimated and it is not mobile. Furthermore, the hill-climbing algorithm is used to increase the estimation accuracy, so Equation 6 is used to create a neighborhood for each particle:

$$X^i(t)=X^i(t-1)+n_d \tag{6}$$

in which n_d is the random variable for randomly creating a neighbor for the previous particle.

• Updating particle weight:

In general, the particle weight is updated based on RSSI. RSSI is a Gaussian variable. Therefore, the path loss can also be Gaussian. Also, the path loss could be formulated using state variables. Therefore, the observation model is written based on the state variables as with Equation 7.

These equations are written for one observation, but three RSSI observations require three reflected signals.

$$\begin{aligned}&(Z(t)\,|\,X^{[i]}(t)=\\&p(PL_{msr(t)}\,|<x^{[i]}(t),y^{[i]}(t),z^{[i]}(t)>)=\\&p(PL_{msr}(t)\,|\,PL_{cal}^{[i]}(t))\end{aligned} \tag{7}$$

in which $PL_{msr}(t)$ is the observed path loss based on RSSI and $PL_{cal}^{[i]}(t)$ is the calculated path loss based on each particle location. This calculated value for each particle is based on Equation 8:

$$PL_{cal}^{[i]} = 91 - 20\log\Gamma(\theta) + 20\log(d_{obs1} + \sqrt{(x^{[i]}(t) - x_{obs1})^2 + (y^{[i]} - y_{obs1})^2 + (z^{[i]} - z_{obs1})^2}) \quad (8)$$

in which x, y, and z are the estimated RF source location, , , and are the reflector location, is the distance between the receiver and reflector that is determined considering the map and reflector location, and θ is the reflection angle that is calculated by Equation 9 using the RF location, reflection location, and receiver location based on the law of cosines.

$$\theta = 90 - \frac{1}{2} * \cos^{-1}(\frac{d_{obs1}{}^2 + ((x^{[i]} - x_{obs1})^2 + (y^{[i]} - y_{obs1})^2 + (z^{[i]} - z_{obs1})^2) - d_r{}^2)}{2d_{obs1}\sqrt{(x^{[i]} - x_{obs1})^2 + (y^{[i]} - y_{obs1})^2 + (z^{[i]} - z_{obs1})^2}}) \quad (9)$$

$$d_r = \sqrt{((x^{[i]} - x_r)^2 + (y^{[i]} - y_r)^2 + (z^{[i]} - z_r)^2}$$

The value of θ can be calculated for every x, y, and z of the RF source location or the dimensions of each particle considering the known UAV location () and obstacle location. Then, this θ value is put in Equation 8, which allows the path loss to be only dependent on the RF location coordinates or the dimensions of each particle. On the other hand, the path loss function is considered a Gaussian distribution function, so the particle weight is updated using Equation 10 considering Equations 6-8:

$$w_t^{[i]}{}_1 = \frac{1}{\sigma_{sh} * \sqrt{2\pi}} e^{-\frac{(PL_{msr1}(t) - PL_{cal_1}^{[i]})^2}{2\sigma_{sh}{}^2}} \quad (10)$$

The particle weight for location estimation in three dimensions is the result of three reflections and their observed weights, which are calculated based on Equation 11:

$$w_t^{[i]} = w_t^{[i]}{}_1 w_t^{[i]}{}_2 w_t^{[i]}{}_3 \quad (11)$$

This operation of weight updating from Equations 6 to 11 is calculated multiple times to execute the hill-climbing algorithm and improve the particle. The new particle weight replaces the older one if it is larger than it. This operation searches the particle's surrounding space to increase its weight.

• Re-Sampling:

There is another sampling after particle weight updating. This is performed using a threshold, which leads to re-sampling if the number of effective particles is lower than it. The normal particle filter calculates the inverse of the total squares of the particle weights as the threshold.

The above particle filter algorithm requires many particles from the beginning for its estimation because of the vast search space and its three-dimensional estimation. This study improves the particle filter algorithm using the KLD criteria, which has been optimized using the bin size to improve the efficiency by which the above problem is estimated.

3- 2- Improving particle filter efficiency in estimating RF source location using the KLD criteria and optimized bin size

This criterion is used in different measurements or the distance between two possible distributions just like Equation 12 [25]:

$$K(p,q) = \sum_x p(x)\log\frac{p(x)}{q(x)} \quad (12)$$

If the probability distributions of p and q are equal, K will be equal to zero; otherwise, it will be a positive number that is not a metric distance and does not have triangular properties.

This criterion requires sample estimation because we do not possess true posterior distribution. The particle filter with KLD can configure the maximum likelihood estimation in a proper range considering the true posterior distribution. In other words, this ML estimation error of sampling method and desired distribution with the probability of 1-δ is lower than ε if the number of particles is equal to or higher than . Equation 13 is to make sure we have this number of particles:

$$N_r = \frac{k-1}{2\varepsilon}(1 - \frac{2}{9(k-1)} + \sqrt{\frac{2}{9(k-1)}} z_{1-\delta})^3 \quad (13)$$

Equation 13 is known as Wilson's theorem and uses a chi-square estimation to obtain the conditions mentioned in KLD. Here, k is the number of bins and z is the highest quantile of the Gaussian distribution. The standard Gaussian distribution tables present this value based on different δs. The value of is easily calculated by knowing these values. The number of bins is determined by the prior distribution and bin sizes. We do not have the prior distribution, so we can consider the number of non-empty bins as the number of k because each particle is allocated to one bin.

The length of each bin in any dimension must be determined because the first figure uses this length as a fixed value during its estimation and the usage of improper lengths can affect the convergence and the estimation accuracy. The length of each bin in any dimension can be determined based on the number of particles according to Equation 14:

$$k_{\max} \approx N_{\max}\varepsilon \quad (14)$$

Equation 14 estimates the number of bins considering the number of particles and estimation accuracy. The known

range of each particle dimension allows for determining the bin dimensions based on the length of each dimension in which the particles are distributed. This is done using Equation 15.

$$(l_{bx}, l_{by}, l_{bz}) = \frac{1}{k_{\max}}(|x_{\min} - x_{\max}|, |y_{\min} - y_{\max}|, |z_{\min} - z_{\max}|) \quad (15)$$

Equation 13 and its parameters have been added to the particle filter considering the large searching space and the need for a high number of particles to obtain an accurate search. The particle number is set at the initial number and their number changes based on Equation 14 during the particle filter iterations to decrease the previous distribution estimation accuracy from ε with the possibility of 1-δ, which improves the localization accuracy. Also, the bin size is determined based on Equation 15, which improves the performance of the particle filter and reduces the calculation complexities using adaptive bin size.

4- Simulation and Results

This section simulates the RF source localization in three dimensions with maps. The signal is assumed to be received using reflection. The UAV moves alongside the signal path to improve the signal-receiving angle measurement. The localization is done in three dimensions based on the map, the known UAV location, and the obstacle location in the signal path. The simulation estimates the RF source location using the map alongside the reflection coefficient, RSSI data, and known reflector location. Also, it is assumed that the UAV receives three reflected signals while moving along a path for search and rescue. The situation of the reflectors compared to each other and the location of these signals can affect the localization accuracy. The localization has been done in four different conditions, and the results are presented here.

The particle filter using the KLD method with an initial minimum of 1500 is distributed evenly considering the large search area to estimate the RF source location. Also, the KLD particle filter has , , and bin length dimensions of 200 meters for x and y alongside 3 meters for the z-axis. These values for the adaptive particle filter change over time based on Equation 14 and each simulation undergoes 200 iterations. In each iteration, the local search is used for each particle five times to improve the localization.

To compare the proposed approach to another approach, because three-dimension localization using RSSI observations and reflection and map was not found in other researches, the advanced approach in the [22] is selected. This approach is localization in 2D using map and reflection in which a simple particle filter is used for estimation and observation is RSSI. 2D localization error is obtained in the 3D environment and it is compared to the error of the localization in 3D with the approach which is proposed in this paper. For a simple particle filter number of particles is constant and equal to 500 which is equal to the mean of particle number in adaptive particle filter.

Figure 5 has three reflectors, allowing the UAV to receive three signals. Multiple geometrical conditions were compared in these simulations. Different values were added to the reflector location dimensions to create new geometrical conditions. Monte-Carlo simulation is run with an average of 100 consecutive runs whose results are presented in Tables 1-4.

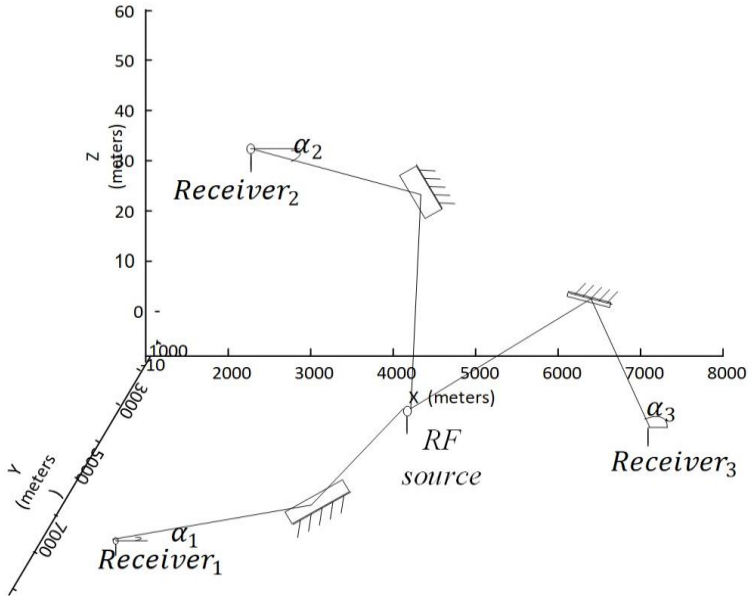

Fig. 5. The locations of the reflectors and receiving point on the simulation environment

Table 1. The RF source localization error in Condition 1 in meters

Condition 1	Noise standard deviation based on dB				
	1	2	3	4	5
RMSE of localization with adaptive KLD PF Filter	*105*	*117*	*144*	*168*	*192*
RMSE of localization with KLD PF	*121*	*128*	*139*	*174*	*208*
RMSE of localization with the approach in[22]	*198*	*221*	*278*	*345*	*365*

Table 2. The RF source localization error in Condition 2 in meters

Condition 2	Noise standard deviation based on dB				
	1	2	3	4	5
RMSE of localization with Adaptive KLD PF	113	136	164	198	221
RMSE of localization with KLD PF	125	140	189	216	231
RMSE of localization with the approach in[22]	185	215	288	320	349

Table 3. The RF source location error in Condition 3 in meters

Condition 3	Noise standard deviation based on dB				
	1	2	3	4	5
RMSE of localization with Adaptive KLD PF	109	128	195	265	291
RMSE of localization with KLD PF	101	134	199	281	311
RMSE of localization with the approach in[22]	256	279	304	367	445

Condition 1: Location of Reflector 1 (3500,5700,35), Location of Reflector 3 (6200,3100,73), and Location of Reflector 2 (2100,3100,170)

Condition 2: Location of Reflector 1 (3200,5800,35), Location of Reflector 3 (4500,3100,73), and Location of Reflector 2 (2100,3100,170)

Condition 3: Location of Reflector 1 (3000,5700,35), Location of Reflector 3 (3500,3100,73), and Location of Reflector 2(2100,3100,170)

Condition 4: Location of Reflector 1 (2800,5400,35), Location of Reflector 3 (3000,3100,73), and Location of Reflector 2 (2100,3100,170)

The estimation accuracy of these four estimations was based on the localization error of those two particle filters and the approach in [22]. The adaptive particle filter with the proper bin size has a better performance and higher estimation speed than the initial KLD particle filter. Also, the locations of two reflectors (Reflectors 1 and 3) were changed in these simulations, and they got closer to each other. This brings the two spheres, which are the geometric locations of the reflectors, closer to one another and increases their noise error compared to when they were more distant from each other. Also, the proposed approach in [22] has more errors

Table 4. The RF source localization error in Condition 4 in meters

Condition 4	Noise standard deviation based on dB				
	1	2	3	4	5
RMSE of localization with Adaptive KLD PF	113	132	201	289	341
RMSE of localization with KLD PF	122	138	194	287	339
RMSE of localization with the approach in [22]	271	315	350	425	496

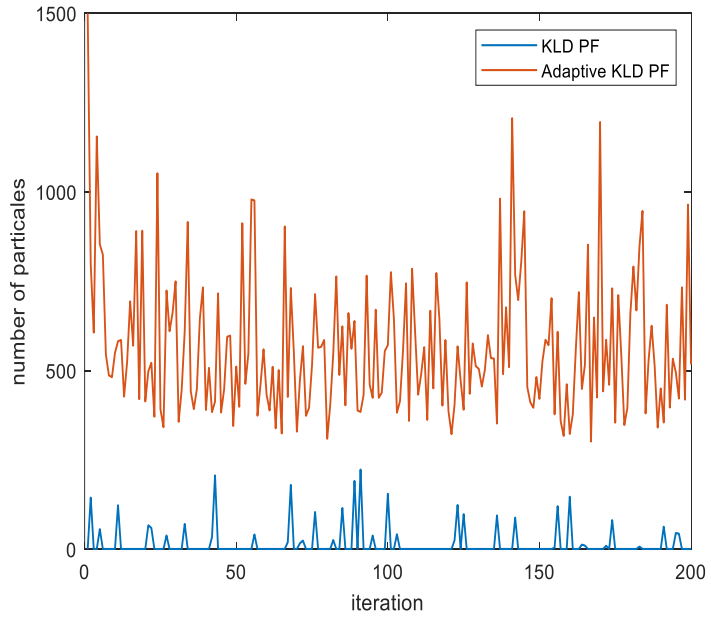

Fig. 6. The number of particles for initial bin dimensions x=150, y=150, z= 1 meter

related to the other method because of using 2D localization equations in 3D environment.

For more investigation, the number of particles for each iteration is shown in Figures 6 and 7. In these figures, it is shown that the length of the bin in each dimension can change the number of particles, and the adaptive bin size can adjust the number of particles for effective estimation. It is hard and time- consuming to determine the bin size in the simple KLD particle filters in three dimensions, and KLD PF for 3D estimation has low performance.

In Figure 6, it is shown that the number of particles for estimation in the KLD PF is low because the size of the bins is not suitable. Also, in Figure 7, the number of particles for the KLD PF is high but estimation has low accuracy because they are not effective.

Based on the above simulations in different locations of the receiving points of reflection, it is shown that localization with particle filter in three dimensions using particle filter is possible and the locations of receiving the reflections have a slight effect on the estimation. Also, the adaptive KLD particle filter has higher accuracy in a large search space using enough particles than the KLD particle filter and the proposed approach in [22] has more errors related to the proposed method of this paper because 2D localization equations are used for 3D environment by a simple particle filter.

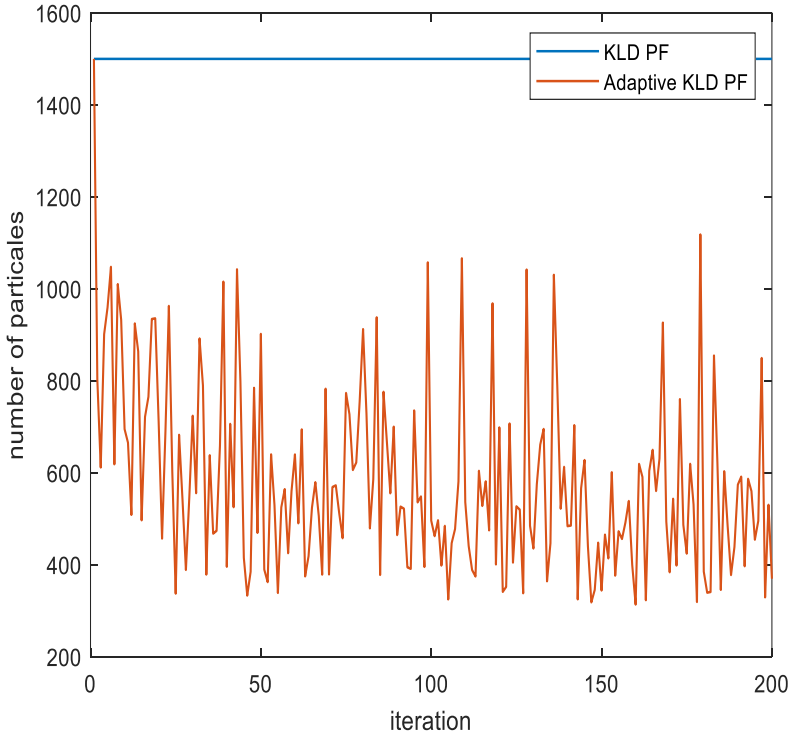

Fig. 7. The number of particles for initial bin dimensions x=250, y=250, z= 5 meter

5- Conclusion

This study performed three-dimensional localization based on signals reflected on obstacles in an outdoor environment. The geometrical location of each reflection based on the estimation information was shown to be a circle in a three-dimensional environment. It was shown analytically and in the simulations that the cross-section of three circles, which were the results of reflected signals, determined the unique RF source location. The KLD criterion and local search were used to improve the particle filter performance for location estimation in 3D. This criterion adaptively selected the number of particles and introduced the bin size as a value based on interval length and the maximum number of particles, which increased the estimation speed and accuracy. The simulation results showed that the adaptive particle filter had a proper speed and accuracy.

References

[1] X. Bai, H. Xu, J. Li, X. Gao, F. Qin, X. Zheng, Coal mine personnel positioning algorithm based on improved adaptive unscented Kalman filter with wireless channel fading and unknown noise statistics, Transactions of the Institute of Measurement and Control, 44(6) (2022) 1217-1227.

[2] A.R. Puji, W.H. Ari, W. Risma, Wireless Nurse Call System Using IoT Implementation, Journal of Electrical and Electronics Engineering, 14(1) (2021) 11-16.

[3] T. Murray, S.F. Hasan, Present state of the art in post disaster victim localization, in: 2020 IEEE 5th International Symposium on Telecommunication Technologies (ISTT), IEEE, 2020, pp. 51-56.

[4] J. Cacace, N. Mimmo, L. Marconi, An ARVA sensor simulator, Robot Operating System (ROS) The Complete Reference (Volume 5), (2021) 233-266.

[5] N. Mimmo, P. Bernard, L. Marconi, Avalanche victim search via robust observers, IEEE Transactions on Control Systems Technology, 29(4) (2020) 1450-1461.

[6] M. Berioli, J.M. Chaves, N. Courville, P. Boutry, J.L. Fondere, H. Skinnemoen, H. Tork, M. Werner, M. Weinlich, WISECOM: A rapidly deployable satellite backhauling system for emergency situations, International Journal of Satellite Communications and Networking, 29(5) (2011) 419-440.

[7] F. Demiane, S. Sharafeddine, O. Farhat, An optimized UAV trajectory planning for localization in disaster scenarios, Computer networks, 179 (2020) 107378.

[8] P. Sinha, I. Guvenc, Impact of antenna pattern on TOA based 3D UAV localization using a terrestrial sensor

network, IEEE Transactions on Vehicular Technology, 71(7) (2022) 7703-7718.

[9] A.T. Le, X. Huang, C. Ritz, E. Dutkiewicz, A. Bouzerdoum, D. Franklin, Hybrid TOA/AOA localization with 1D angle estimation in UAV-assisted WSN, in: 2020 14th International Conference on Signal Processing and Communication Systems (ICSPCS), IEEE, 2020, pp. 1-6.

[10] S. Tomic, M. Beko, R. Dinis, P. Montezuma, Distributed algorithm for target localization in wireless sensor networks using RSS and AoA measurements, Pervasive and Mobile Computing, 37 (2017) 63-77.

[11] K. Yu, I. Sharp, Y.J. Guo, Ground-based wireless positioning, John Wiley & Sons, 2009.

[12] Q. Tian, Y. Liu, Q. Hu, A NLOS Mitigation Algorithm for TOA Based Localization in Mixed LOS/NLOS Environments, in: International Conference on Autonomous Unmanned Systems, Springer, 2022, pp. 2843-2853.

[13] Y. Wang, K. Gu, Y. Wu, W. Dai, Y. Shen, NLOS effect mitigation via spatial geometry exploitation in cooperative localization, IEEE Transactions on Wireless Communications, 19(9) (2020) 6037-6049.

[14] C. Gentner, T. Jost, W. Wang, S. Zhang, A. Dammann, U.-C. Fiebig, Multipath assisted positioning with simultaneous localization and mapping, IEEE Transactions on Wireless Communications, 15(9) (2016) 6104-6117.

[15] S. Haidari, H. Moradi, M. Shahabadi, S.M. Dehghan, A reflection-based rf source localization algorithm, International Journal of Robotics and Automation, 34(3) (2019).

[16] S. Haidari, H. Moradi, M. Shahabadi, S.M. Dehghan, RF source localization using reflection model in NLOS condition, in: 2016 4th International Conference on Robotics and Mechatronics (ICROM), IEEE, 2016, pp. 601-606.

[17] M. Zaidi, I. Bouazzi, M. Usman, M.Z. Mohammed Shamim, N. Singh, V.K. Gunjan, Cooperative Scheme ToA-RSSI and Variable Anchor Positions for Sensors Localization in 2D Environments, Complexity, 2022 (2022).

[18] R. Zekavat, R.M. Buehrer, Handbook of position location: Theory, practice and advances, John Wiley & Sons, 2011.

[19] X. Chu, Z. Lu, D. Gesbert, L. Wang, X. Wen, Vehicle localization via cooperative channel mapping, IEEE Transactions on Vehicular Technology, 70(6) (2021) 5719-5733.

[20] X. Zhang, L. Chen, M. Feng, T. Jiang, Toward reliable non-line-of-sight localization using multipath reflections, Proceedings of the ACM on Interactive, Mobile, Wearable and Ubiquitous Technologies, 6(1) (2022) 1-25.

[21] Y. Wang, K. Zhao, Z. Zheng, A 3D indoor positioning method of wireless network with single base station in multipath environment, Wireless Communications and Mobile Computing, 2022 (2022).

[22] S. Haidari, H. Moradi, S. Dehghan, RF source localization using obstacles map and reflections, International Journal of Industrial Electronics Control and Optimization, 4(2) (2021) 181-190.

[23] A.W. Li, G.S. Bastos, A hybrid self-adaptive particle filter through KLD-sampling and SAMCL, in: 2017 18th International Conference on Advanced Robotics (ICAR), IEEE, 2017, pp. 106-111.

[24] H. Budiarto, K. Horihata, K. Haneda, J.-i. Takada, Experimental study of non-specular wave scattering from building surface roughness for the mobile propagation modeling, IEICE transactions on Communications, 87(4) (2004) 958-966.

[25] T. Li, S. Sun, T.P. Sattar, Adapting sample size in particle filters through KLD-resampling, Electronics Letters, 49(12) (2013) 740-742.

HOW TO CITE THIS ARTICLE

S. Haidari, A. Hosseinpour, Three-Dimensional RF Source Localization Using Reflection and an Improved Particle Filter, AUT J. Elec. Eng., 55(3) (Special Issue) (2023) 365-376.

DOI: 10.22060/eej.2023.22102.5512